



Advances in COD Equations – Multiple Loading Modes: Validation of the Analytical Models to Experimental Data

Andrew J. Cox¹, Bruce A. Young², and Paul M. Scott³

¹Research Scientist, Battelle Memorial Institute, Columbus, OH (CoxA@battelle.org)

²Principal Research Scientist, Battelle Memorial Institute, Columbus, OH

³Research Leader, Battelle Memorial Institute, Columbus, OH

ABSTRACT

Non-linear fracture mechanics equations for through-wall cracks (TWC) in a pipe are used to analyze nuclear piping systems for either critical flaw size or critical loading conditions as part of probabilistic Leak-Before-Break (LBB) failure analyses. These probabilistic codes use a large number of independent solutions to determine an overall assessment of system failure probability. For each individual realization, if a TWC is determined to be present, the solution requires an estimation of the crack opening displacement (COD) for the postulated TWC as part of a leak rate evaluation.

Updated analytical COD equations have been proposed in Young *et al.* (2012) and Young *et al.* (2013). These updated equations were based on the GE-EPRI formulation for COD found in Kumar, V. and German, M. D. (1988) and Rahman *et al.* (1998-1,2,3). The updated solutions utilized significant advancements in computational capability and speed, such that, structural finite element analyses (FEA) were completed using three-dimensional 20-node continuum brick elements. The results of the FEA provided the basis to determine analytical functions which incorporate axial load due to internal pressure, crack face pressure, and applied bending moment for a solution which provides through-thickness variations in COD for a wide range of normalized crack lengths and pipe R/t ratios.

While validation of the analytical equations to non-linear FEA have been provided in the previously published papers such as Young *et al.* (2012) and Young *et al.* (2013), this paper focuses on the validation of the analytical solutions to experimental results. For the experimental data, a suite of experiment results ranging from pure tension to tension plus bending were used from the Pipe Fracture Database developed in Wilkowski *et al.* (1995).

INTRODUCTION

As computational memory and speed increase, LBB evaluations in the nuclear piping industry have transitioned from a deterministic basis to a probabilistic framework. Thus, accurately characterizing the best-estimate leak rate has become increasingly important. As LBB evaluations become more refined, the ability for standardized leak rate codes, such as the Seepage Quantification of Upsets in Reactor Tubes (SQUIRT) code (Paul *et al.* (1994)), to accept through-thickness variations in crack-opening displacement (COD) values has become more common.

As a result of the limitations with the existing GE-EPRI type methods for predicting COD values for TWCs in pipes, such as limitation of crack size, fixed pressure for combined pressure and bending solutions, and no through thickness variation in COD, the development of a comprehensive COD prediction tool for combined loadings applicable to a wide range of piping systems was undertaken. To provide solutions more close to actual plant applications, the loading assumption in the present work is that the axial load (due to internal pressure) and the crack face pressure are prescribed concurrently with the moment being applied subsequent to the internal pressure.

Prior to the validation work completed on this project, the most recently published research works in the area of determining analytical solutions for COD are provided by Kumar and German (1988), Rahman

et al. (1998-1,2,3), Rudland *et al.* (2002), Young *et al.* (2012), and Young *et al.* (2013). Young *et al.* (2013) provides an overview of the technical basis for the equations being validated in this paper.

THEORY

While the detailed theory of the COD equations for through-wall cracks in a pipe is provided in Young *et al.* (2013), some of the equations are shown in this section for completeness. The loading assumption is that the axial load (due to internal pressure) and the crack face pressure are applied concurrently with the moment applied subsequent to the internal pressure. Unlike previous solutions, there is no restriction that the pressure be a fixed, predetermined value.

For axial loading of a pipe with a through-wall crack (TWC), a failure surface approach for the loading condition of concurrent axial load (due to pressure in an end-capped pipe) (P_{ip}) and crack face pressure (P_{CFP}) was proposed as shown in Equation 1. The limit load (P_o) (i.e. the load at which the un-cracked ligament becomes a fully plastic hinge) for a pipe with a through-wall crack under axial load is given in Equation 2 as a function of the yield stress (σ_o), the mean radius of the pipe (R_m), the pipe thickness (t), and the half-crack size in radians (θ).

$$\frac{P_{CFP}}{P_o} + \frac{P_{ip}}{P_o} = 1 \quad (1)$$

$$P_o = 2\sigma_o R_m t \left\{ \pi - \theta - 2\sin^{-1} \left[\frac{1}{2} \sin(\theta) \right] \right\} \quad (2)$$

Since the crack face pressure is equal to the internal pressure on the inner diameter of the pipe and zero on the outer diameter of the pipe, a first order approximation was made such that the crack face pressure is equal to a linear fraction of the internal pressure (γp_i). The far-field stress value ($\sigma_{(T)}^\infty$), due to the combined internal pressure and crack face pressure, to calculate the elastic COD is provided in Equation 3 as a function of the internal pressure (p_i), the mean radius of the pipe (R_m), the inner radius of the pipe (R_i), the pipe thickness (t), the fraction of the internal pressure (γ) with the assumption of no externally applied axial loads.

$$\sigma_{(T)}^\infty = \frac{p_i R_i^2}{2R_m t} + \gamma p_i \quad (3)$$

To mimic the behavior in a physical nuclear piping system, an assumption was made that the internal pressure and the crack face pressure were applied concurrently; such that, the load ratio (λ) given in Equation 4 is constant for a given crack size and pipe geometry. Thus, Equation 1 can then be rewritten as Equation 5.

$$\lambda = \left(\frac{P_{CFP}}{P_{ip}} \right) = \left[\frac{2\gamma\theta R_m t}{\pi R_i^2} \right] \quad (4)$$

$$\frac{\lambda P_{ip}}{P_o} + \frac{P_{ip}}{P_o} = 1 \quad (5)$$

Using a failure surface approach, the load ratio, λ , and the load due to the internal pressure, P_{ip} , an effective limit-load expression is derived and shown in Equation 6.

$$P'_o = \frac{P_o}{1 + \lambda} \quad (6)$$

The GE-EPRI formulation for the analytical COD equations separates the elastic and plastic solutions as shown in Equation 7. If we assume the axial load comes from the internal pressure on an end-capped pipe with a through-wall crack, the total displacement equation is Equation 8 provided by Young *et al.* (2012). To satisfy continuity, when the crack face pressure is zero (i.e., $\gamma = 0$), the equation must collapse to GE-EPRI Equation. Thus, the plastic influence functions for the solution with crack face pressure must be equal to the plastic influence functions without crack face pressure. Values for the plastic influence function, h_2^T , and the elastic influence functions, $V_{1(T)}$, are provided in Young *et al.* (2012). The solution in Equation 8 is expressed as functions of half crack length (a), Young's modulus (E), reference strain (ϵ_o), Ramberg-Osgood fitting coefficient (α), and the Ramberg-Osgood strain-hardening exponent (n).

$$\delta_{(total)}^T = \delta_{(T)}^{el} + \delta_{(T)}^{pl} \quad (7)$$

$$\delta_{(total)}^{(T+CFP)} = \frac{4a}{E} \left[\left(\frac{R_i^2}{2R_m t} + \gamma \right) p V_{1(T)} \right] + \alpha \epsilon_o a h_2^T \left[\frac{P_{ip}(1 + \lambda)}{P_o} \right]^n \quad (8)$$

Since there are differences between long through-wall cracks and short through-wall cracks, mainly consisting of the in-plane rotation under pressure, adjustments are required to the analytical solution. The first adjustment is a fitting term as a function of the normalized crack length. For short cracks the pipe neutral axis is outside the crack plane, while for long cracks the pipe neutral axis is inside the crack plane. This difference creates a phenomenon which requires crack opening corrections for the crack face pressure portion of the equation (f_1).

The second adjustment is due to the way the analytical solutions for the GE-EPRI model are derived (i.e. under the small scale yielding assumption). When finite element calculations are performed to compensate for relatively large displacement phenomenon, which provides a closer approximation to reality, the rotation the cap-ended pipe is increased. Thus, a second fitting term based on the strain hardening parameter is required for a reduction in analytic model to finite element error (f_2). Recasting the elastic-plastic solution with the correction factors is shown in Equation 9.

$$\delta_{(total)}^T = \frac{4a}{E} \left[\left(\frac{R_i^2}{2R_m t} + \gamma \right) f_2 p V_{1(T)} \right] + \alpha \epsilon_o a h_2^T f_2 \left[\frac{P_{ip}(1 + \lambda f_1)}{P_o} \right]^n \quad (9)$$

As discussed earlier for the axial load solution, a similar correction is required for the bending moment to correct for the difference between small strain solutions and large strain solution (f_3). Since the effect of elastic stresses can be added linearly, the total elastic COD is then given by Equation 10; and, the plastic COD due to tension is given in Equation 11. The details of the correction factors can be found in Young *et al.* (2013).

$$\delta^{(el)} = \frac{4a}{E} \left[\left(\frac{R_i^2}{2R_m t} + \gamma \right) f_2 p V_{1(T)} + f_3 \frac{M_{app} R_m}{I} V_{1(B)} \right] \quad (10)$$

$$\delta_{(Tension)}^{(pl)} = \alpha \varepsilon_o a h_2^T f_2 \left[\frac{P_{ip}(1 + \lambda f_1)}{P_o} \right]^n \quad (11)$$

A concept of equivalent moment is now introduced. This equivalent moment (M_{eq}) is the moment required to obtain the same plastic COD in Equation 11. For reference, the limit moment (M_o) (i.e. the moment at which the un-cracked ligament becomes a fully plastic hinge) for a pipe with a through-wall crack under moment loading is given in Equation 12. The equivalent moment is then determined using the plastic COD equation given in Young *et al.* (2012) and recasting it as Equation 13.

$$M_o = 4\sigma_o R_m^2 t \left[\cos\left(\frac{\theta}{2}\right) - \frac{1}{2} \sin(\theta) \right] \quad (12)$$

$$M_{eq} = M_o \left[\frac{\delta_{(Tension)}^{(pl)}}{f_3 \alpha \varepsilon_o a h_2^B} \right]^{(1/n)} \quad (13)$$

Once the equivalent moment is determined for the plastic COD due to tension, a total effective moment (M_{eff}) can be calculated using the equivalent moment (M_{eq}) and the applied moment (M_{app}) as shown in Equation 14. Equation 15 provides the final solution in terms of the GE-EPRI method of the elastic COD plus the plastic COD.

$$M_{eff} = M_{eq} + M_{app} \quad (14)$$

$$\delta_{(total)} = \frac{4a}{E} \left[\left(\frac{R_i^2}{2R_m t} + \gamma \right) f_2 p V_{1(T)} + f_3 \frac{M_{app} R_m}{I} V_{1(B)} \right] + f_3 \alpha \varepsilon_o a h_2^B \left[\frac{M_{eff}}{M_o} \right]^n \quad (15)$$

The details of the validation of Equation 15 to experimental data are provided in the next section.

VALIDATION

Seven full-scale pipe test experiments from the Pipe Fracture Database, developed by Wilkowski *et al.* (1995), were used as a comparison to validated Equation 15. Two sets of analyses were performed; one using the raw data and Equation 15 directly and a second using a correction factor for Equation 15 as a function of strain hardening exponent. Detailed characterization of the pipe experiments can be found in Table 1.

Table 1. Characteristics of the Circumferential Through-Wall Crack Experiments

Specimen ID		4131-1	4121-1	4111-6	111-24	4111-2	111-26	1-8
Base Material		304 SS	304 SS	A516 Gr70 / CS	SA 333 Gr6 / CS	A155-KC60 / CS	316L SS	A106 Gr-B / CS
Weld		No	No	No	Yes	No	No	No
OD	(mm)	166.4	168.1	910.1	612.0	711.0	106.2	399.3
Wall	(mm)	13.4	12.9	72.84	31.3	23.6	8.3	26.2
θ/π		0.370	0.386	0.370	0.079	0.37	0.244	0.120
Temperature	(C)	287.8	287.8	287.8	287.8	287.8	21	287.8
Internal Pressure	(MPa)	17.235	Increase	0	0	0	0	15.5
Gamma		0	0	0	0	0	0	1
R_m/t		5.71	6.02	5.75	9.28	14.6	5.9	7.12
Yield	(MPa)	139.0	139.0	210.0	229.0	231.0	254.0	216.5
UTS	(MPa)	450.0	450.0	510.0	525.0	544.0	532.0	506.1
Alpha		9.69	9.69	2.07	2.14	1.15	5.50	2.37
N		3.13	3.13	5.20	4.36	5.55	4.76	4.03
E	(GPa)	182.9	182.9	206.3	200.0	206.3	157.5	206.3
σ_f	(MPa)	294.5	294.5	360.0	377.0	387.5	393.0	361.1
Span (Inner)	(mm)	1220	N/A	3350	3350	3350	610	3350
Span (Outer)	(mm)	3200	N/A	11580	11580	11580	1524	11580
R_o	(mm)	83.2	84.1	455.1	306.0	355.5	53.1	199.7
R_m	(mm)	76.5	77.6	418.6	290.4	343.7	49.0	186.6
R_i	(mm)	69.8	71.2	382.2	274.7	331.9	44.8	173.5
Test Type IP – Increasing Pressure FP – Fixed Pressure 4B – 4pt Bend		FP + 4B	IP	4B	4B	4B	4B	FP +4B

Direct Comparison

To determine if any experimental-factor correction was required to be applied to Equation 15, an initial comparison was made to the seven experiments shown in Table 1. The results of the initial comparison are shown in Figure 1. Based on this comparison and similar results obtained by Kim *et al.* (2001) and Kim *et al.* (2002) an experimental correction factor was developed.

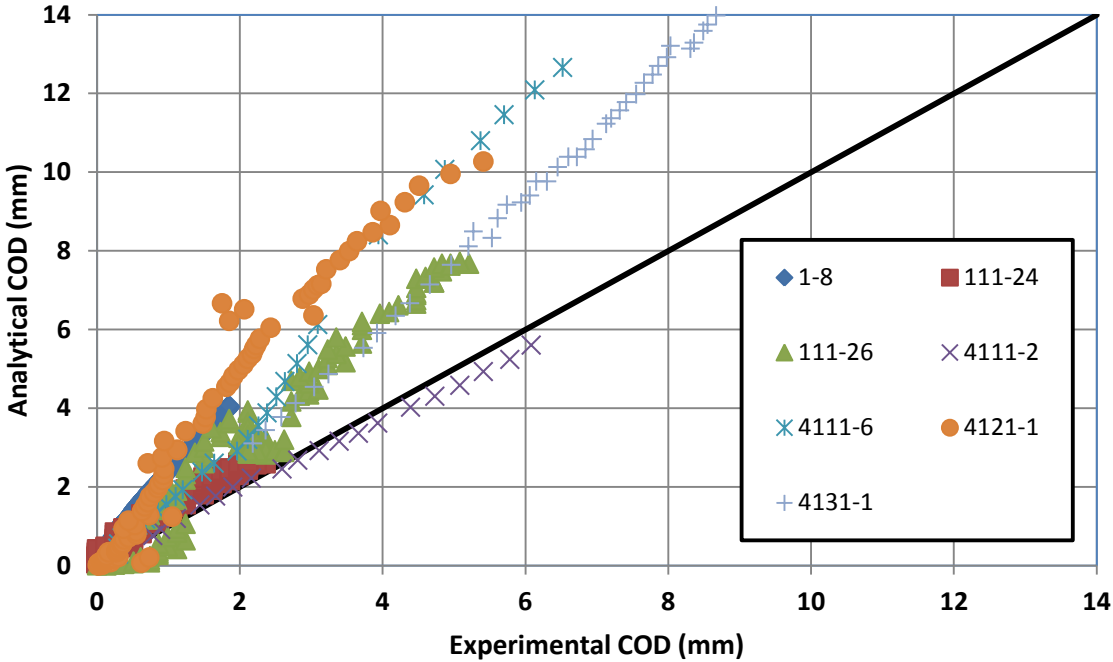


Figure 1. Comparison of Equation 15 to the Experimental Data

Corrected Comparison

The analysis of data involved reviewing the contributions of elastic COD and plastic COD provided by Equation 15. Based on this review, the correction factor (f_4) provided in Equation 16 was implemented. A new set of plastic COD equations was implemented for the plastic COD portions as shown in Equations 17 through 19 with Equation 19 being the final solution implemented in the updated *CALC_COD* software.

$$f_4 = 1.15 \quad (16)$$

$$\delta_{(Tension)}^{(pl)} = \left(\frac{1}{f_4}\right)^n \alpha \varepsilon_o a h_2^T f_2 \left[\frac{P(1 + \lambda f_1)}{P_o}\right]^n \quad (17)$$

$$M_{eq} = f_4 M_o \left[\frac{\delta_{(Tension)}^{(pl)}}{f_3 \alpha \varepsilon_o a h_2^B}\right]^{(1/n)} \quad (18)$$

$$\delta_{(total)} = \left\{ \frac{4a}{E} \left[\left(\frac{R_i^2}{2R_m t} + \gamma \right) f_2 p V_{1(T)} + f_3 \frac{M_{app} R_m}{I} V_{1(B)} \right] + \left(\frac{1}{f_4} \right)^n f_3 \alpha \varepsilon_o a h_2^B \left[\frac{M_{eff}}{M_o} \right]^n \right\} \quad (19)$$

While separating the experimental correction factor (f_4) from the base equations as shown in Equations 17 through 19 was the method shown here, the net effect of this correction is increasing the limit moment and limit load by 15 percent (i.e. increasing the effective yield strength by 15 percent). Using Equation 19, the data for the experiments shown in Table 1 were used for validation. Figure 2 shows the results of the final validation of Equation 19. As can be seen in comparing Figures 1 and 2, the agreement between the analytical CODs and the experimental CODs is much better when this correction factor (f_4) is used.

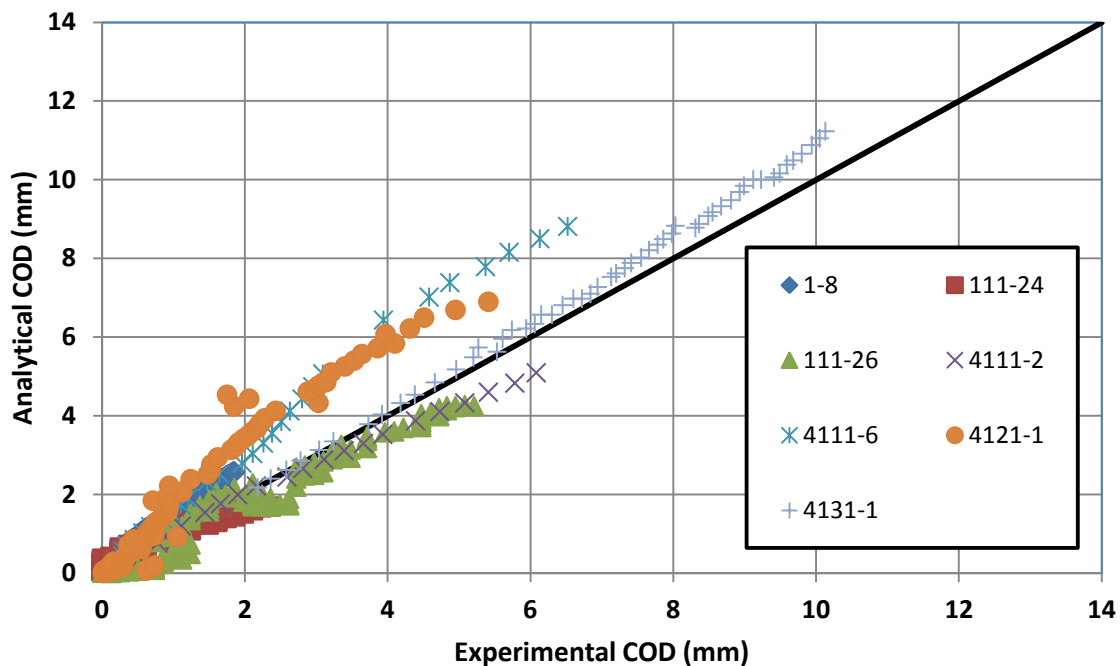


Figure 2. Comparison of Equation 19 to the Experimental Data

CONCLUSIONS

The work reported in this paper is a validation of the research by Young *et al.* (2012) and Young *et al.* (2013) with experimental results. Several key elements to provide a validation of the analytical solution are provided.

The following items are a list of key conclusions from this portion the current study.

- Based on work in Young *et al.* (2013), the COD functions are dependent on the rotation characteristics provided by the boundary conditions. Functions to compensate for the crack size as well as the rotation as a function of material characteristics have been developed and implemented.

- Based on work in this study, validation has been completed for the given solution and implemented in the updated CALC_COD subroutine. This includes the experimental correction factor provided in this paper in Equation 16.
- With respect to the final solution, the solution estimates the COD for a pipe which is free to rotate at the ends. In reality, the pipe is restrained at the pipe-ends which in turn causes smaller COD values than reported. Together with the current leak-rate software, this may cause a non-conservative result with respect to pipe rupture probabilities. Application of restraint of pressure induced bending results should be investigated such as found in Rahman, S. *et al.* (1998-3), Kim *et al.* (2007), Olson *et al.* (2003), and Feng *et al.* (2001).

ACKNOWLEDGMENTS

This work was conducted at Battelle Columbus as part of the NRC’s Piping Integrity Program. The authors would like to thank the NRC’s Office of Research for their support of this program.

NOMENCLATURE

P_{ip}	Axial Load due to Internal Pressure	M_o	Collapse Bending Moment
P_{CFP}	Axial Load due to Internal Pressure	γ	Crack face pressure to internal pressure ratio
P_o	Collapse Tension Force	λ	Load Ratio
σ_o	Reference Stress	δ	COD
R_m	Mean Pipe Radius	$\delta^{(el)}$	Elastic COD
t	Pipe Thickness	$\delta^{(pl)}$	Plastic COD
θ	Crack Angle (total crack angle = 2θ)	a	Crack Length (total length = $2a$)
R_i	Inner Radius of Pipe	n	Strain Hardening Exponent
p_i	Internal Pipe Pressure	α	Strength Coefficient
p_{CF}	Crack Face Pressure	ϵ_o	Reference Strain
$\sigma_{(T)}^\infty$	Far-Field Tension Stress	h_2	Plastic Influence Function
A	Cross-Section of Pipe	E	Young’s Modulus
P_A	Applied Axial Far-Field Force	V_1	Elastic Influence Function
M_{app}	Applied Bending Moment	$V_{1(T)}$	Elastic Influence Function for Tension
M_{eq}	Equivalent Bending Moment	$V_{1(B)}$	Elastic Influence Function for Bending
M_{eff}	Effective Bending Moment ($M_{eq} +$	I	Second Moment of Inertia for a Pipe

REFERENCES

- Feng, Z., Miura, N., Ghadiali, N., Brust, F., Santos, T., Choi, J.B., Park, C.Y., and Wilkowski, G. (2001). “Effects of Pipe-System Restraint on COD Calculations of Axial Loaded Pipes for LBB Applications – Finite Element Round Robin Results,” Structural Mechanics in Reactor Technology (SMiRT) 16, Washington, DC
- Kim, J.-W. (2007). “Evaluation Model for Restraint Effect of Pressure Induced Bending on the Plastic Crack Opening of a Circumferential Through-Wall Crack,” Nuclear Engineering Technology, Vol. 39, No. 1, pp. 75-84.

- Kim, Y.-J., Huh, N.S., and Kim, Y.-J. (2001). “Enhanced reference stress based J and COD estimation method for LBB analysis and comparison with GE/EPRI method,” Fatigue Fract Engng Mater Structure, Vol. 24, pp. 243-254.
- Kim, Y.-J., Huh, N.S., and Kim, Y.-J. (2002). “Reference stress based elastic-plastic fracture analysis for circumferential through-wall cracked pipes under combined tension and bending,” Engineering Fracture Mechanics, Vol. 69, pp. 367-388.
- Kumar, V. and German, M.D. (1988). “Elastic-Plastic Fracture Analysis of Through-Wall and Surface Flaws in Cylinders,” EPRI Report NP-5596, Research Project 1237-5
- Paul, D.D., Ahmad, J., Scott, P.M., Flanigan, L.F., and Wilkowski, G.M. (1994). “Evaluation and Refinement of Leak-Rate Estimation Models,” NUREG/CR-5128, BMI-2164 Rev. 1, June 1994
- Olson, R.J., Morbitzer, R.A., Scott, P.M., and Wilkowski, G.M. (2003) “Practical Application of Restraint of Pressure-Induced Bending Phenomenon in Leak Rate Calculations,” Structural Mechanics in Reactor Technology (SMiRT) 17, Prague, Czech Republic
- Rahman, S., Brust, F.W., Ghadiali, N., and Wilkowski, G.M. (1998-1). “Crack-Opening-Area Analyses for Circumferential Through-wall Cracks in Pipes – Part I: Analytical Models,” International Journal of Pressure Vessels and Piping, Vol. 75, pp. 357-373.
- Rahman, S., Brust, F.W., Ghadiali, N., and Wilkowski, G.M. (1998-2). “Crack-opening-area analyses for circumferential through-wall cracks in pipes – Part II: model validations,” International Journal of Pressure Vessels and Piping, Vol 75 (1998), pp. 375-396.
- Rahman, S., Ghadiali, N., Wilkowski, Moberg, F., and Brickstad, B. (1998-3). “Crack-opening-area analyses for circumferential through-wall cracks in pipes – Part III: off-center cracks, restraint of bending, thickness transitions and weld residual stresses,” International Journal of Pressure Vessels and Piping, Vol 75 (1998), pp. 397-415.
- Rudland, D.L., Wang, Y.-Y., and Wilkowski, G.M. (2002). “Comparison of crack-opening predictions for LBB applications,” International Journal of Pressure Vessels and Piping, Vol. 79, pp. 209-217
- Wilkowski, G.M., Ghadiali, N., Rudland, D., Keishnaswamy, P., Rahman, S., and Scott, P. (1995) “Short Cracks in Piping and Pipe Welds: Seventh Program Report March 1993 – December 1994,” NUREG/CR-4599, BMI-2173, Vol. 4, No. 1.
- Young, B.A., Olson, R.J., and Kerr, M. (2012). “Advances in COD Modeling: Circumferential Through-Wall,” ASME International, PVP 2012, PVP2012-78181, Toronto, ON, Canada
- Young, B.A., Olson, R.J., and Scott, P.M. (2013) “Advances in COD Equations – Multiple Loading Modes: Concurrent Axial and Crack Face Pressure Loading with a Subsequent Applied Bending Moment,” Structural Mechanics in Reactor Technology (SMiRT) 22, San Francisco, CA